

Syntheses and Structures of Two Metal-organic Frameworks Constructed from Zn/Ni and 3-Formyl-4-(pyridin-4-yl) Benzoic Acid Ligand

ANNEES ABBAS⁽¹⁾;ZHANG Jie⁽¹⁾ (张杰);LI Zi-Jian⁽¹⁾ (李子建);LIU Yan⁽¹⁾ (刘燕);LIU

Bai-Zhan⁽²⁾(刘百战);CUI Yong⁽¹⁾ (崔勇)

⁽¹⁾ State Key Laboratory of Metal Matrix Composites; School of Chemistry and Chemical Engineering, Shanghai Jiaotong University, Shanghai 200240, China;⁽²⁾China Tobacco, Shanghai 200240, China

ABSTRACT Two metal-organic frameworks $[(\text{Zn}_{0.5}\text{L})(\text{H}_2\text{O})]_n$ (**1**) and $[(\text{Ni}_{0.5}\text{L})(\text{H}_2\text{O})]_n$ (**2**) constructed by the 3-formyl-4-(pyridin-4-yl) benzoic acid ligand (**HL**) were synthesized and characterized by single-crystal X-ray diffraction. **1** crystallizes in orthorhombic space group *Pnna* with $a = 16.6152(8)$, $b = 12.6825(6)$, $c = 15.3908(8)$ Å, $V = 3243.2(3)$ Å³, $Z = 4$, $M_r = 511.12$, $D_c = 1.047$ g/cm³, $F(000) = 1048$, $\mu = 1.144$ mm⁻¹, $GOOF = 1.061$, the final $R = 0.0471$ and $wR = 0.1262$ for 12168 observed reflections with $I > 2\sigma(I)$. **2** is isostructural to **1**, which also crystallizes in orthorhombic space group *Pnna* with $a = 16.6152(8)$, $b = 12.6825(6)$, $c = 15.3908(8)$ Å, $V = 3243.2(3)$ Å³, $Z = 4$, $M_r = 511.12$, $D_c = 1.047$ g/cm³, $F(000) = 1048$, $\mu = 1.144$ mm⁻¹, $GOOF = 1.061$, the final $R = 0.0471$ and $wR = 0.1262$ for 12168 observed reflections with $I > 2\sigma(I)$. Additionally, thermogravimetric analysis, FT-IR spectroscopy and powder X-ray diffraction were discussed.

Keywords: metal-organic frameworks;crystal structure; Zn; Ni; formyl

DOI: 10.14102/j.cnki.0254-5861.2011-1712

1 INTRODUCTION

Metal-organic frameworks (MOFs) as a novel class of crystalline porous materials have drawn much attention for the last decades^[1-15]. MOFs are being actively studied for various applications such as gas storage and separation, catalysis, proton conduction, environmental monitoring, chemical sensing, ion exchange, drug delivery, *etc.*^[16-26].

To organize molecules in 3D space, metal-organic frameworks (MOFs) are excellent pile materials. Installing complex functional moieties into the MOF skeleton led to rapid elaboration of MOF diversity. Postsynthetic modification (PSM) is also a powerful method of tuning MOF composition, functionality, and porosity. It is becoming increasingly important to develop MOFs possessing functionality that can modify the pore or bring in sophisticated properties. Postsynthetic modification (PSM) represents an attractive strategy of functionalization^[27]. Particularly attractive, the organic component of MOFs can be prefabricated to contain a specific reactive group (tag), and then rational covalent PSM may be performed via the diverse organic reactions developed by organic chemists. More approaches of PSM are still being sought to enrich the diversity and complexity of MOFs and to achieve better performance and new functions^[28]. However, there is a dilemma in the study: on the one hand, the group chosen to a tag MOF should not coordinate to the metal ion and should be stable enough to survive the synthetic conditions of MOF; on the other hand, most MOFs have limited chemical stability, so the tag should be active enough to allow PSM under mild conditions without destroying the MOF structure.

A possible limitation for the study is the chemical lability of the aldehyde group, which could be incompatible with the synthetic reactions for MOFs^[29]. Here we report the synthesis of aldehyde-tagged MOFs **1** and **2** by the direct solvothermal reaction. MOFs **1** and **2** were constructed by the 3-formyl-4-(pyridin-4-yl) benzoic acid ligand and characterized by single-crystal X-ray diffraction, thermogravimetric analysis, FT-IR spectroscopy and powder X-ray diffraction^[30].

2 EXPERIMENTAL

2.1 Materials and apparatus

The ligand 4-bromo-3-formylbenzoic acid (HL) was synthesized according to the procedure of literature^[30]. The ligand 3-formyl-4-(pyridin-4-yl) benzoic acid was synthesized in 65% yield by a palladium-catalyzed Suzuki coupling reaction between 4-pyridylboronic and 4-bromo-3-formylbenzoic acids. Other chemicals were commercially available, and used without further purification. The FT-IR (KBr pellet) spectra were recorded (400~4000 cm⁻¹ region) on a Nicolet Magna 750 FT-IR spectrometer. TGA was carried out in a N₂ atmosphere at a heating rate of 10 °C min⁻¹ on a STA449C integration thermal analyzer. Powder X-ray diffraction (PXRD) data were collected on a Bruker D8 Advance diffractometer using CuK α radiation at 40 kV, 40 mA power.

2.2 Syntheses of **1** and **2**

2.2.1 Synthesis of **1**

A mixture of $\text{Zn}(\text{NO}_3)_2 \cdot 6\text{H}_2\text{O}$ (8.9 mg, 0.03 mmol), 3-formyl-4-(pyridin-4-yl) benzoic acid (6.8 mg, 0.03 mmol), DMF (1 mL), and EtOH (0.5 mL) in a capped vial was heated at 80 °C for 48 h. Prismatic crystals of **1** were filtered, washed with MeOH and Et_2O , respectively and dried at room temperature. Yield: 29.3 mg (69%) based on $[(\text{Zn}_{0.5}\text{L}) (\text{H}_2\text{O})]_n$. Anal. Calcd. for $[(\text{Zn}_{0.5}\text{L}) (\text{H}_2\text{O})]_n$: C, 56.38; H, 3.64; N, 5.06%. Found: C, 56.40; H, 3.57; N, 5.10%.

FT-IR (KBr pellet, ν/cm^{-1}): 472 (m), 642 (w), 766 (m), 780 (s), 815 (m), 837 (m), 946 (m), 1010 (m), 1098 (m), 1192 (m), 1224 (m), 1243 (m), 1296 (m), 1374 (s), 1424 (s), 1554 (m), 1618 (s), 1699 (s), 2750 (w), 2860 (w), 2974 (w), 3065 (w).

2. 2. 2 Synthesis of 2

A mixture of $\text{Ni}(\text{NO}_3)_2 \cdot 6\text{H}_2\text{O}$ (8.7 mg, 0.03 mmol), 3-formyl-4-(pyridin-4-yl) benzoic acid (6.8 mg, 0.03 mmol), DMF (1 mL), and EtOH (0.5 mL) in a capped vial was heated at 80 °C for 48 h. Blue prismatic crystals of **2** were filtered, washed with MeOH and Et_2O respectively, and dried at room temperature. Yield: 25.9 mg (61%), based on $[(\text{Zn}_{0.5}\text{L}) (\text{H}_2\text{O})]_n$. Anal. Calcd. for $[(\text{Zn}_{0.5}\text{L}) (\text{H}_2\text{O})]_n$: C, 57.07; H, 3.68; N, 5.12%. Found: C, 57.10; H, 3.75; N, 5.20%.

FT-IR (KBr pellet, ν/cm^{-1}): 472 (m), 648 (w), 766 (m), 784 (s), 821 (m), 838 (m), 948 (m), 1010 (w), 1100 (m), 1193 (m), 1224 (m), 1250 (m), 1303 (w), 1386 (s), 1420 (s), 1438 (s), 1529 (m), 1549 (m), 1581 (s), 1610 (s), 1697 (s), 2756 (w), 2848 (w), 2933 (w), 3185 (w), 3409 (w).

2. 3 Crystallographic measurements

Single-crystal XRD data for **1** and **2** were collected on a Bruker APEX-II CCD diffractometer with graphite-monochromatic $\text{CuK}\alpha$ radiation ($\lambda = 1.54178 \text{ \AA}$) at 123(2) K. The structure was solved and refined by direct methods with SHELXS-2014 and refined with SHELXL-2014³¹ using *OLEX 2.0*³². All the non-hydrogen atoms were refined by full-matrix techniques with anisotropic displacement parameters and the hydrogen atoms were geometrically fixed at the calculated positions attached to their parent atoms, and treated as riding atoms. Contributions to scattering due to these highly disordered solvent molecules were removed using the *SQUEEZE* routine of *PLATON* (Spek, A. L. *J. Appl. Crystallogr.* **2003**, 36, 7); Structures were then refined again using the data generated. For **1** (CCDC-1547814), the final $R = 0.0471$ and $wR = 0.1262$ ($w = 1/[\sigma^2(F_o^2) + (0.1071P)^2]$, where $P = (F_o^2 + 2F_c^2)/3$), $S = 1.061$, $(\Delta/\sigma)_{\text{max}} = 0.001$, $(\Delta\rho)_{\text{max}} = 0.199$ and $(\Delta\rho)_{\text{min}} = -0.288 \text{ e}/\text{\AA}^3$. For **2** (CCDC-1547815), the final $R = 0.0471$ and $wR = 0.1262$ ($w = 1/[\sigma^2(F_o^2) + (0.1071P)^2]$, where $P = (F_o^2 + 2F_c^2)/3$), $S = 1.061$, $(\Delta/\sigma)_{\text{max}} = 0.001$, $(\Delta\rho)_{\text{max}} = 0.199$ and $(\Delta\rho)_{\text{min}} = -0.288 \text{ e}/\text{\AA}^3$.

The selected bond lengths and bond angles are given in Tables 1 and 2, respectively.

Table 1. Selected Bond Lengths (Å) and Bond Angles (°) for 1

Bond	Dist.	Bond	Dist.	Bond	Dist.
Zn(1)–O(1)#1	2.0457(15)	Zn(1)–O(1)	2.0457(15)	Zn(1)–O(2)#1	2.3223(17)
Zn(1)–O(2)	2.3223(17)	Zn(1)–N(1)#2	2.0599(19)	Zn(1)–N(1)#3	2.0599(19)
Angle	(°)	Angle	(°)	Angle	(°)
O(1)#1–Zn(1)–O(1)	148.50(10)	O(1)#1–Zn(1)–O(2)#1	60.28(6)	O(1)–Zn(1)–O(2)#1	94.56(6)
O(1)–Zn(1)–O(2)	60.28(6)	O(1)#1–Zn(1)–O(2)	94.56(6)	O(1)#1–Zn(1)–N(1)#2	97.80(7)
O(1)–Zn(1)–N(1)#3	97.80(7)	O(1)–Zn(1)–N(1)#2	101.34(7)	O(1)#1–Zn(1)–N(1)#3	101.34(7)
N(1)#2–Zn(1)–O(2)#1	155.33(7)	N(1)#3–Zn(1)–O(2)	155.33(7)	N(1)#3–Zn(1)–O(2)#1	91.73(7)
N(1)#2–Zn(1)–O(2)	91.73(7)	N(1)#2–Zn(1)–N(1)#3	104.51(11)	O(2)–Zn(1)–O(2)#1	79.84(9)

Symmetry transformation: #1 $-x+1/2, -y+1, z$; #2 $-x+1, y+1/2, z+1/2$; #3 $x-1/2, -y+1/2, z+1/2$; #4 $x+1/2, -y+1/2, z-1/2$

Table 2. Selected Bond Lengths (Å) and Bond Angles (°) for 2

Bond	Dist.	Bond	Dist.	Bond	Dist.
Ni(1)–O(1)	2.056(3)	Ni(1)–O(2)	2.157(3)	Ni(1)–O(2)#1	2.157(3)
Ni(1)–N(1)#2	2.030(4)	Ni(1)–N(1)#3	2.030(4)	Ni(1)–O(1)#1	2.056(3)
Angle	(°)	Angle	(°)	Angle	(°)
O(1)–Ni(1)–O(1)#1	157.4(2)	O(1)#1–Ni(1)–O(2)#1	63.00(13)	O(1)#1–Ni(1)–O(2)	99.36(13)
O(1)–Ni(1)–O(2)#1	99.36(13)	O(1)–Ni(1)–O(2)	63.00(13)	O(2)#1–Ni(1)–O(2)	83.82(18)
N(1)#2–Ni(1)–O(1)#1	97.81(15)	N(1)#3–Ni(1)–O(1)	97.82(15)	N(1)#2–Ni(1)–O(1)	96.93(15)
N(1)#3–Ni(1)–O(1)#1	96.93(15)	N(1)#3–Ni(1)–O(2)#1	158.51(14)	N(1)#2–Ni(1)–O(2)#1	92.61(14)
N(1)#2–Ni(1)–O(2)	158.51(14)	N(1)#3–Ni(1)–O(2)	92.60(14)	N(1)#3–Ni(1)–N(1)#2	98.1(2)

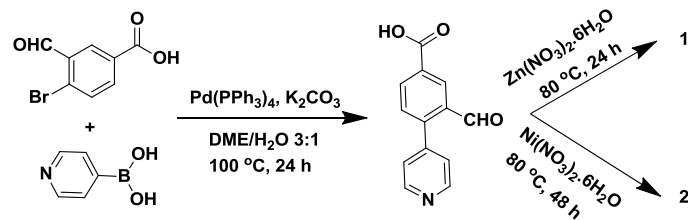
Symmetry transformation: #1 $-x+1/2, -y+1, z$; #2 $x-1/2, -y+1/2, z+1/2$; #3 $-x+1, y+1/2, z+1/2$; #4 $x+1/2, -y+1/2, z-1/2$

3 RESULTS AND DISCUSSION

3.1 Synthesis and characterization of 1 and 2

As shown in Scheme 1, the ligand 3-formyl-4-(pyridin-4-yl) benzoic acid was synthesized in 65% yield based on 4-bromo-3-formylbenzoic acid by a palladium-catalyzed Suzuki coupling reaction between 4-pyridylboronic and 4-bromo-3-formylbenzoic acids. **1** and **2** were obtained by solvothermal reactions between Zn(II), Ni(II) ions and 3-formyl-4-(pyridin-4-yl) benzoic acid, respectively. Their phase purity was confirmed by experimental and simulated X-ray powder diffraction patterns. After the removal of guest solvents by solvent exchange followed by thermal activation under vacuum at 80 °C, **1** and **2** still retained their frameworks indicated by powder XRD (Fig. 1). As shown in Fig. 2, products **1** and **2** show a strong band at ~ 1690 cm⁻¹, characteristic of aldehyde $\nu(\text{C}=\text{O})$. According to thermogravimetric analysis (Fig. 3), materials **1** and **2** release solvent molecules upon heating to 200 °C. The framework starts to decompose at

about 350 °C.



Scheme 1. Syntheses of 1 and 2

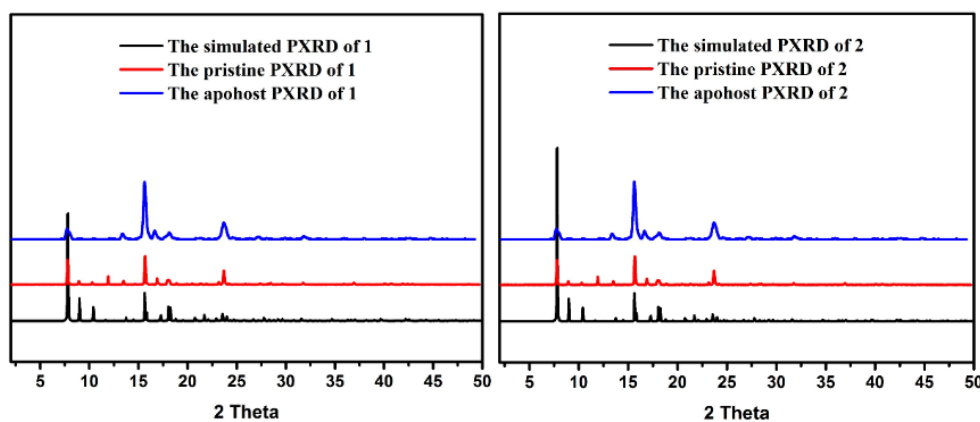


Fig. 1. Simulated and experimental PXRD patterns of 1 and 2

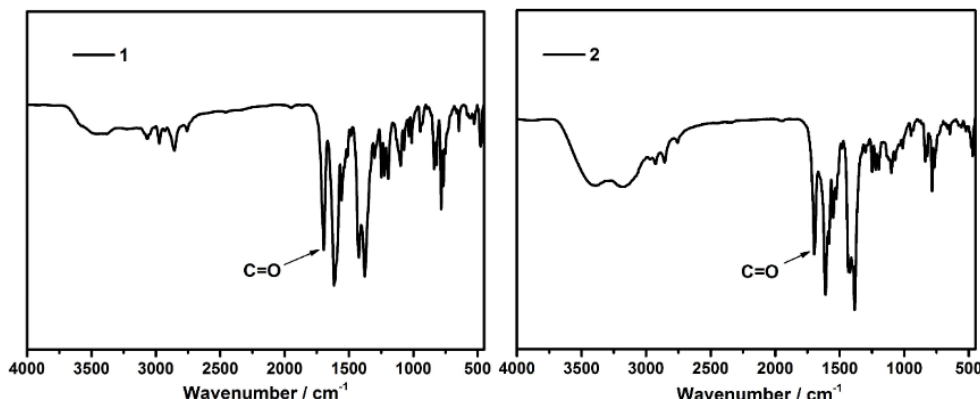


Fig. 2. IR spectra of 1 and 2

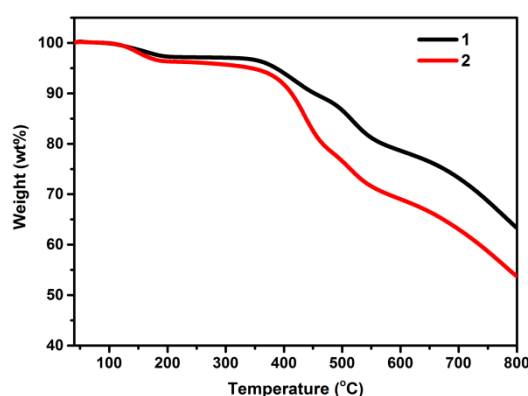
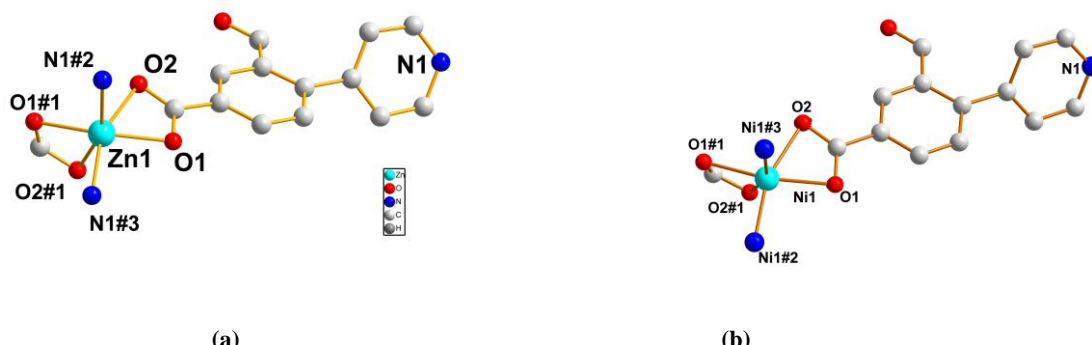


Fig 3. Thermal analysis curves of **1** and **2**

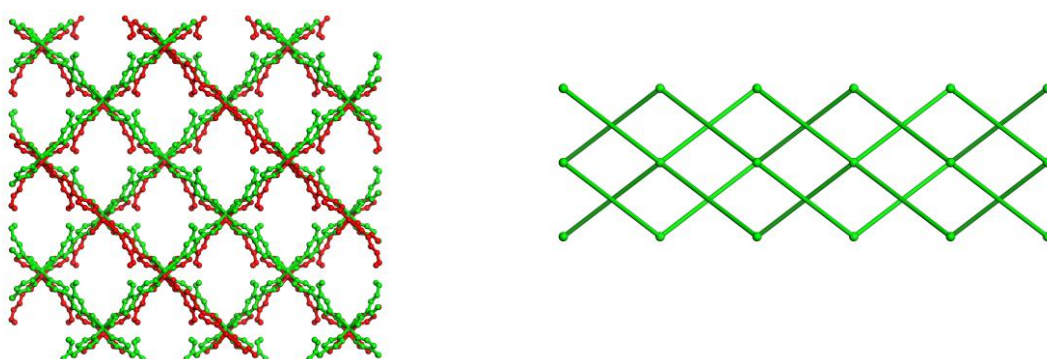
3.2 Structural descriptions

1 crystallizes in the orthorhombic space group *Pnna* with the asymmetric unit consisting of half a Zn(II) ion and one 3-formyl-4-(pyridin-4-yl) benzoic acid ligand. The Zn ion exhibits a distorted octahedral environment supplied by N atoms of pyridine moieties of two ligands with the Zn–N bond length of 2.0599(19) Å and two chelated carboxylate groups of two ligands with the Zn–O bond lengths ranging from 2.0457(15) to 2.3223(17) Å, as shown in Fig. 4a. The lengths of Zn–N and Zn–O are within the range reported for Zn(II) based coordination polymers^[33]. And each ligand connects two Zn(II) centers (Fig. 4b). Thus, each Zn in **1** is linked by four ligands and each ligand is linked to two Zn to generate a 3D diamond network. Two kinds of these 3D networks interpenetrate with each other to generate the final framework.

Isostructural to **1**, **2** also crystallizes in the orthorhombic space group *Pnna* with the Ni–N bond length of 2.030(4) Å and the Ni–O bond lengths ranging from 2.056(3) to 2.157(4) Å, which are within the range reported for Ni(II) based coordination polymers^[34-41].

**Fig. 4.** Coordination modes for Zn(II) in **1** (a) and Ni(II) in **2** (b)

Hydrogen atoms and guest molecules are omitted for clarity



a**b****Fig. 5. 2-fold-interpenetrated nets (a) and the simplified topology (b) in 1**

4 CONCLUSION

In conclusion, we have synthesized two new metal-organic frameworks with zinc and nickel based on the 3-formyl-4-(pyridin-4-yl) benzoic acid, respectively. They have been characterized by the single-crystal, powder X-ray diffraction, FT-IR and TGA. In addition, the active aldehyde group in the two MOFs provides a versatile and convenient “handle” for PSM and the study is underway.

chinaXiv:201711.00146v1

REFERENCES

- (1) Deria, A.; Gomez-Gualdon, D. A.; Hod, I.; Snurr, R. Q.; Hupp, J. T.; Farha, O. K. Framework-topology-dependent catalytic activity of zirconium based (porphinato) zinc(II) MOFs. *J. Am. Chem. Soc.* **2016**, *138*, 14449–14457.
- (2) Chen, Q.; Sun, J.; Li, P.; Hod, I.; Moghadam, P. Z.; Kean, Z. S.; Snurr, R. Q.; Hupp, J. T.; Farha, O. K.; Stoddart, J. F. A redox-active bistable molecular switch mounted inside a metal–organic framework. *J. Am. Chem. Soc.* **2016**, *138*, 14242–14245.
- (3) Kundu, A.; Piccini, G. M.; Sillar, K.; Sauer, J. *Ab initio* prediction of adsorption isotherms for small molecules in metal–organic frameworks. *J. Am. Chem. Soc.* **2016**, *138*, 14047–14056.
- (4) Lu, W.; Wei, Z.; Gu, Z.; Liu, T.; Park, J.; Park, J.; Tian, J.; Zhang, M.; Zhang, Q.; Gentle, T.; Bosch, M.; Zhou, H. C. Tuning the structure and function of metal-organic frameworks via linker design. *Chem. Soc. Rev.* **2014**, *43*, 5561–5593.
- (5) Silva, P.; Vilela, S. M. F.; Tome, J. P. C.; Almeida Paz, F. A. Multifunctional metal-organic frameworks from academia to industrial applications. *Chem. Soc. Rev.* **2015**, *44*, 6774–6803.
- (6) Dhakshinamoorthy, A.; Asiri, A. M.; Garcia, H. Metal-organic frameworks catalyzed C–C and C–heteroatom coupling reactions. *Chem. Soc. Rev.* **2015**, *44*, 1922–1947.
- (7) Zhang, T.; Lin, W. Metal-organic frameworks for artificial photosynthesis and photocatalysis. *Chem. Soc. Rev.* **2014**, *43*, 5982–5993.
- (8) Stavila, V.; Talin, A. A.; Allendorf, M. D. MOF-based electronic and opto-electronic devices. *Chem. Soc. Rev.* **2014**, *43*, 5994–6010.
- (9) Schneemann, A.; Bon, V.; Schwedler, I.; Senkovska, I.; Kaskel, S.; Fischer, R. A. Flexible metal-organic frameworks. *Chem. Soc. Rev.* **2014**, *43*, 6062–6096.
- (10) Lin, Z.; Lu, J.; Hong, M.; Cao, R. Metal-organic frameworks based on flexible ligands (FL-MOFs): structures and applications. *Chem. Soc. Rev.* **2014**, *43*, 5867–5895.
- (11) Li, M.; Li, D.; O’Keeffe, M.; Yaghi, O. M. Topological analysis of metal–organic frameworks with polytopic linkers and/or multiple building units and the minimal transitivity principle. *Chem. Rev.* **2014**, *114*, 1343–1370.
- (12) Hu, Z.; Deibert, B. J.; Li, J. Luminescent metal-organic frameworks for chemical sensing and explosive detection. *Chem. Soc. Rev.* **2014**, *43*, 5815–5840.
- (13) Li, H.; Niu, Z.; Han, T.; Zhang, Z.; Shi, W.; Cheng, P. A microporous lanthanide metal-organic framework containing channels: synthesis, structure, gas adsorption and magnetic properties. *Sci. China Chem.* **2011**, *54*, 1423–1429.
- (14) Zhang, X.; Yang, Q.; Zhao, J.; Hu, T.; Chang, Z.; Bu, X. Three interpenetrated copper(II) coordination polymers based on a V-shaped ligand: synthesis, structures, sorption and magnetic properties. *Sci. China Chem.* **2011**, *54*, 1446–1453.
- (15) Wei, Z.; Yuan, D.; Zhao, X.; Sun, D.; Zhou, H. Linker extension through hard-soft selective metal coordination for the construction of a

non-rigid metal-organic framework. *Sci. China Chem.* **2013**, 56, 418-422.

(16) Liu, Y.; Xuan, W.; Cui, Y. Engineering homochiral metal-organic frameworks for heterogeneous asymmetric catalysis and enantioselective separation. *Adv. Mater.* **2010**, 22, 4112-4135.

(17) Yoon, M.; Srirambalaji, R.; Kim, K. Homochiral metal-organic frameworks for asymmetric heterogeneous catalysis. *Chem. Rev.* **2012**, 112, 1196-1231.

(18) Peluso, P.; Mamane, V.; Cossu, S. Homochiral metal-organic frameworks and their application in chromatography enantioseparations. *J. Chromatogr. A* **2014**, 1363, 11-26.

(19) Peng, Y.; Gong, T.; Zhang, K.; Lin, X.; Liu, Y.; Jiang, J.; Cui, Y. Engineering chiral porous metal-organic frameworks for enantioselective adsorption and separation. *Nat. Commun.* **2014**, 5.

(20) Wanderley, M. M.; Wang, C.; Wu, C.; Lin, W. A chiral porous metal-organic framework for highly sensitive and enantioselective fluorescence sensing of amino alcohols. *J. Am. Chem. Soc.* **2012**, 134, 9050-9053.

(21) Ye, C.; Zhu, C.; Gong, T.; Shen, E.; Xuan, W.; Cui, Y.; Liu, B. A novel Cu-based metallosalan complex: synthesis, structure and chiral sensor study. *Chin. J. Struct. Chem.* **2013**, 32, 1076-1082.

(22) Ma, L.; Falkowski, J. M.; Abney, C.; Lin, W. A series of isoreticular chiral metal-organic frameworks as a tunable platform for asymmetric catalysis. *Nat. Chem.* **2010**, 2, 838-846.

(23) Mo, K.; Yang, Y.; Cui, Y. A homochiral metal-organic framework as an effective asymmetric catalyst for cyanohydrin synthesis. *J. Am. Chem. Soc.* **2014**, 136, 1746-1749.

(24) Zhu, C.; Yuan, G.; Chen, X.; Yang, Z.; Cui, Y. Chiral nanoporous metal-metallosalen frameworks for hydrolytic kinetic resolution of epoxides. *J. Am. Chem. Soc.* **2012**, 134, 8058-8061.

(25) Xi, W.; Liu, Y.; Xia, Q.; Li, Z.; Cui, Y. Direct and post-synthesis incorporation of chiral metallosalen catalysts into metal-organic frameworks for asymmetric organic transformations. *Chem. Eur. J.* **2015**, 21, 12581-12586.

(26) Zhang, F.; Zhou, Y.; Dong, J.; Liu, B.; Zheng, S.; Cui, Y. Synthesis and crystal structure of a novel chiral 3D metal-organic framework based on an N-methyl substitutedsalan ligand. *Chin. J. Struct. Chem.* **2014**, 33, 1154-1158.

(27) Cohen, S. M. Postsynthetic methods for the functionalization of metal-organic frameworks. *Chem. Rev.* **2012**, 112, 970-1000.

(28) Gui, B.; Meng, X.; Chen, Y.; Tian, J.; Liu, G.; Shen, C.; Zeller, M.; Yuan, D.; Wang, C. Reversible tuning hydroquinone/quinone reaction in metal-organic framework: immobilized molecular switches in solid state. *Chem. Mater.* **2015**, 27, 6426-6431.

(29) Liu, C.; Luo, T. Y.; Feura, E. S.; Zhang, C.; Rosi, N. L. Orthogonal ternary functionalization of a mesoporous metal-organic framework via sequential postsynthetic ligand exchange. *J. Am. Chem. Soc.* **2015**, 137, 10508-10511.

(30) Williams, D. E.; Dolgopolova, E. A.; Pellechia, P. J.; Palukoshka, A.; Wilson, T. J.; Tan, R.; Maier, J. M.; Greytak, A. B.; Smith, M. D.; Krause, J. A.; Shustova, N. B. Mimic of the green fluorescent protein β -barrel: photophysics and dynamics of confined chromophores defined by a rigid porous scaffold. *J. Am. Chem. Soc.* **2015**, 137, 2223-2226.

(31) Sheldrick, G. M. *SHELXT-2014*, 2013.

(32) Dolomanov, O. V.; Bourhis, L. J.; Gildea, R. J.; Howard, J. A. K.; Puschmann, H. *J. Appl. Crystallogr. ScienceOpen. Inc.* **2009**, 42, 339-341.

(33) Zhang, J.; Li, Z.; Gong, W.; Han, X.; Liu, Y.; Cui, Y. Chiral DHIP-based metal-organic frameworks for enantioselective recognition and separation. *Inorg. Chem.* **2016**, 55, 7229-7232.

(34) Müller, P.; Bon, V.; Senkovska, I.; Getzschmann, J.; Weiss, M. S.; Kaskel, S. Crystal engineering of phenylenebis(azanetriyl)tetrabenzoate based metal-organic frameworks for gas storage applications. *Cryst. Growth Des.* **2017**, 17, 3221-3228.

(35) Zhou, H. C.; Long, J. R.; Yaghi, O. M. Introduction to metal-organic frameworks. *Chem. Rev.* **2012**, 112, 673.

(36) Kim, M.; Cahill, J. F.; Prather, K. A.; Cohen, S. Postsynthetic modification at orthogonal reactive sites on mixed, bifunctional metal-organic frameworksw. *Chem. Commun.* **2011**, 47, 7629-7631.

(37) Furukawa, H.; Cordova, K. E.; O'Keeffe, M.; Yaghi, O. M. Minerals with metal-organic framework structures. *Science* **2013**, 341, 1230444.

(38) Burnett, B. J.; Barron, P. M.; Hu, C.; Choe, W. Stepwise synthesis of metal-organic frameworks: replacement of structural organic linkers. *J. Am. Chem. Soc.* **2011**, 133, 9984-9987.

(39) Mehlana, G.; Susan, A.; Ramon, B. G. A new class of thermo- and solvatochromic metal-organic frameworks based on 4-(pyridin-4-yl)benzoic acid.

Dalton Trans. **2012**, *41*, 4224–423.

(40) Evans, O. R.; Lin, W. Crystal engineering of nonlinear optical materials based on interpenetrated diamondoid coordination networks. *Chem. Mater.* **2001**, *13*, 2705–2712.

(41) Elsaidi, S. K.; Mohamed, M. H.; Wojtas, L.; Chanthapally, A.; Pham, T.; Space, B.; Vittal, J. J.; Zaworotko, M. J. Putting the squeeze on CH₄ and CO₂ through control over interpenetration in diamondoid nets. *J. Am. Chem. Soc.* **2014**, *136*, 5072–5077.

Syntheses and Structures of Two Metal-organic Frameworks Constructed from Zn/Ni and 3-Formyl-4-(pyridin-4-yl) Benzoic Acid Ligand

ANNEES ABBAS ZHANG Jie(张杰) LI Zi-Jian(李子建)

LIU Yan(刘燕) LIU Bai-Zhan(刘百战) CUI Yong(崔勇)

The synthesis, structure and thermal stability of 3-formyl-4-(pyridin-4-yl) benzoic acid based zinc and nickel frameworks **1** and **2** were reported. In **1**, each zinc is linked by four 3-formyl-4-(pyridin-4-yl) benzoic acid ligands, and each 3-formyl-4-(pyridin-4-yl) benzoic acid ligand is linked to two zinc atoms to generate a 3D network; In **2**, each nickel is linked by four 3-formyl-4-(pyridin-4-yl) benzoic acid ligands, and each 3-formyl-4-(pyridin-4-yl) benzoic acid ligand is linked to two nickel clusters to generate a 3D network.

